

Human Bed Nucleus of the Stria Terminalis Indexes Hypervigilant Threat Monitoring

Leah H. Somerville, Paul J. Whalen, and William M. Kelley

Background: Though a key symptom underlying many anxiety disorders is hypervigilant threat monitoring, its biological bases in humans remain poorly understood. Animal models suggest that anxious processes such as hypervigilant threat monitoring are distinct from cued fear-like responses and mediated by the bed nucleus of the stria terminalis (BNST). Here, we applied psychophysiological and neuroimaging methodologies sensitive to sustained arousal-based responses to test the role of the human BNST in mediating environmental threat monitoring, a potential experimental model for sustained anxiety symptoms.

Methods: Healthy participants ($n = 50$) with varying trait anxiety performed an environmental threat-monitoring task during functional magnetic resonance imaging where a stimulus line continuously fluctuated in height, providing information relevant to subsequent risk for electric shocks. Skin conductance was collected in a separate cohort ($n = 47$) to validate task-evoked modulation of physiological arousal.

Results: A forebrain region consistent with the BNST showed greater overall recruitment and exaggerated tracking of threat proximity in individuals with greater anxiety. The insular cortex tracked threat proximity across all participants, showed exaggerated threat proximity responding with greater anxiety, and showed enhanced recruitment when threat proximity was ostensibly controllable.

Conclusions: Activity in the BNST and insula continuously monitored changes in environmental threat level and also subserved hypervigilant threat-monitoring processes in more highly trait anxious individuals. These findings bridge human and animal research informing the role of the BNST in anxious-related processes. In addition, these findings suggest that continuous functional magnetic resonance imaging paradigms offer promise in further elucidating the neural circuitries supporting sustained anticipatory features of anxiety.

Key Words: Anxiety, bed nucleus of stria terminalis, emotion, fMRI, insula, vigilance

A primary aspect of anxious behavior, and a key symptom of anxiety disorders, is chronic, nonspecific apprehension and arousal related to the potential occurrence of future threats (1,2). In clinical populations, levels of apprehension are often inappropriate given environmental demands, leading to tension, worry, behavioral impairments, and distress (3,4). Anxious apprehension is distinct from exaggerated cue-evoked responses to potential threats such as a phobic individual encountering their most feared stimulus (5,6). Such cued responses are triggered readily and exaggerated in magnitude but tend to subside over time when the fear-evoking stimulus is no longer present. Anxious apprehension, by contrast, can fluctuate in magnitude over an extended time scale and be triggered in the absence of discrete, fear-evoking cues. One manifestation of anxious apprehension is hypervigilance, defined as an enhanced state of arousal and readiness to deal with potential threats, often accompanied by negative affect states and activation of the autonomic nervous system (7). Psychologically, hypervigilance is characterized by heightened monitoring of the environment for cues related to one's future level of threat or safety (8,9).

Seminal work using the animal model has dissociated profiles of transient and sustained threat processing that map onto the constructs of fear and anxiety (10,11). In rodents, the presence of an unambiguous, proximal predator elicits the classically characterized fear response (12,13). As the distance from a predator increases or if the predator's presence is ambiguous, these

discrete behaviors give way to sustained risk assessment and vigilance (12). Neurobiologically, cued threat processing is initiated by the amygdala, whereas sustained vigilance associated with ambiguous or distant threat cues is represented by tonic engagement of the bed nucleus of the stria terminalis (BNST), a ventral basal forebrain structure located superior, medial, and rostral to the amygdala (11,14–18). Recently, elevated resting metabolism within the BNST has been identified to mediate trait anxious temperament in primates (19,20) and BNST lesions disrupt individual variability in rodent anxiety-like behavior (21). Taken together, these data motivate the hypothesis that the neurobiological bases of hypervigilant threat monitoring in humans may also be more BNST-dependent and less amygdala-dependent, distinguishing this form of affective processing from the extensive literature implicating the amygdala in cued responses to discrete threats.

Presently, human neuroimaging experiments poised to inform our understanding of hypervigilant threat monitoring are rare, as most experimental paradigms evaluate responses to discrete stimuli. Meta-analyses have identified a network of brain regions including the amygdala, insular cortex, medial prefrontal cortex, and anterior cingulate that are consistently engaged while processing discrete affective cues including facial expressions, negative images, and conditioned stimuli (22,23). Additionally, individuals with anxiety disorders elicit exaggerated responses in several of these regions when encountering discrete affective cues (24,25).

By contrast, we developed a task in which arousal is continuously modulated along temporally slow parameters while subjects monitor the environment for cues signaling risk for a forthcoming aversive event. During functional magnetic resonance imaging (fMRI) scanning and skin conductance recording, participants viewed a stimulus line that fluctuated in height, and if the line exceeded a marked threshold, they would accumulate an electric shock that they believed would be administered later. This rendered the experiment free of cued, transient affective

From the Department of Psychological and Brain Sciences, Dartmouth College, Hanover, New Hampshire.

Address correspondence to Leah H. Somerville, Ph.D., Weill Cornell Medical College, 1300 York Avenue, Box 140, New York, NY 10065; E-mail: lhs2003@med.cornell.edu.

Received Dec 22, 2009; revised Apr 6, 2010; accepted Apr 6, 2010.

events. Variation in the height of the line comprised a dynamic representation of future environmental threat level, validated with skin conductance data to evoke greater arousal with increasing proximity to the shock threshold. We targeted the ventral basal forebrain (VBF), which includes the human BNST, to test whether responses increased with greater threat level and were biased toward exaggerated activity in anxious individuals. Finally, we assessed whether controllability modulated these effects (17,26) by including one condition where participants believed the line represented their physiological responding and a second line was thought to be outside of their volitional control.

Methods and Materials

Participants

One hundred seven subjects participated in one of two experiments. Forty-eight subjects underwent skin conductance recording and 59 separate subjects completed fMRI scanning. In the fMRI sample, seven participants were excluded for movement exceeding 2 mm and/or signal artifacts, and two participants were excluded for suspicion of the cover story (disbelief they could be shocked), leaving a final sample of $n = 50$ (22 male participants, mean age = 19.1). One participant from the skin conductance sample was excluded due to suspicion of the cover story, leaving a final sample of $n = 47$ (22 male participants, mean age = 18.9). Setup, recording, and analysis of the skin conductance sample are reported in Supplement 1. This research was conducted in accordance with guidelines of the Committee for the Protection of Human Subjects at Dartmouth College and all participants provided informed written consent.

Prescreening

Participants were verified to be absent of clinically diagnosable levels of current anxiety disorders and current or past mood disorders using the Structured Clinical Interview for DSM-IV Axis I Disorders (27) and no participant was using psychotropic medications. The potential for covarying mood effects was minimized by excluding any participant scoring greater than 10 on the Beck Depression Inventory (28). The fMRI participants reported no abnormal neurological history, were native speakers of English, and were verified right-handed with the Edinburgh Handedness Inventory (29).

Anxiety Characterization

Participants completed several self-report indexes including the Spielberger State-Trait Anxiety Inventory (30), Behavioral Inhibition/Activation Scale (31), NEO Personality Inventory Neuroticism and Extraversion subscales (32), Intolerance of Uncertainty (33), Penn State Worry Questionnaire (34), Anxiety Symptom Index (35), and Beck Depression Inventory (28). It was reasoned that several scales assessing a range of anxiety symptoms would more comprehensively represent participants' general anxiety level than any scale alone. When evaluating the range of anxiety scores against population norms using the Spielberger State-Trait Anxiety Inventory Trait scale (30), scores in the fMRI cohort ranged from the 1st to 85th percentile with a mean percentile of 39 (SD = 22.7; median = 38) and the galvanic skin response (GSR) cohort ranged from the 1st to 99th percentile with a mean percentile of 38 (SD = 27.56; median = 40). A principal components analysis was conducted with standard parameters (36), inputting self-report measures, to identify latent metavariables representing general anxiety. Results identified two factors (Table S1 in Supplement 1). Scales indexing general

anxiety loaded on the first factor, which explained 45.13% of variance in the overall dataset. Component scores were extracted and used as a single representation of participants' dispositional anxiety in subsequent analyses. The second factor explained 13.3% of variance representing extraversion and was not analyzed further.

Task

During fMRI scanning, participants viewed videos of a line fluctuating in height over time, which they believed represented either their own real-time physiological state (self line [SELF]), ostensibly recorded via a pulse oximeter attached to their finger (Supplementary Methods in Supplement 1 for details regarding stimuli and setup). To test for effects of whether the threat was supposedly controllable, we included a passive line-viewing condition where subjects ostensibly viewed a prerecorded physiological time course of another subject who had previously completed the experiment (other line [OTHER]). Lines were, in fact, created by experimenters but appeared to resemble physiological responses using actual recording software (Figure S1 in Supplement 1). For both conditions, participants were instructed they would accumulate electric shocks that would be delivered after the task whenever the line exceeded a certain threshold (horizontal blue line). An updated tally of the number of accumulated shocks was viewable on the right side of the screen (Figure 1).

Participants were instructed that during one scan (SELF), they would passively view their own physiological responses in real time and should try to stay calm and avoid accumulating shocks. When viewing the other line (OTHER), they were to passively view the other person's performance, realizing that any shocks accrued by the prior subject would also be delivered at the conclusion of the experiment. To circumvent the use of discrete threat, we stated that we would measure how much time they spent above the blue line and would give them the shocks they

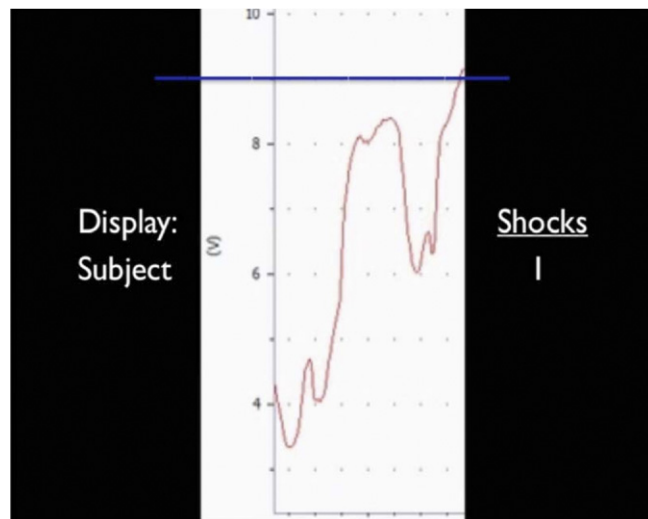


Figure 1. Representative screenshot of task stimulus. Stimuli consisted of a fluctuating line (red) that continuously advanced across the screen from right to left. The stationary blue line represented the height above which participants would accumulate an electric shock to be delivered later. On the right is a continuous tally of how many shocks had been accumulated. On the left is a label of whether the presented ostensibly represented the participant's own internal state information (Subject) or a prerecording of another individual's internal state information (Other), which the participant was to passively view.

had accumulated after the task was complete. To facilitate believability of the cover story, participants underwent a shock workup procedure in the control room and wore a faux shocking apparatus in the scanner (Supplementary Methods in Supplement 1).

fMRI

Imaging was performed on a Philips Intera Achieva 3.0 Tesla scanner with a SENSE head coil (both Philips Medical Systems, Bothell, Washington). Two T2* weighted scans sensitive to the blood oxygenation level-dependent contrast (repetition time = 2000 msec, echo time = 35 msec, flip angle = 90°, 3 × 3 in-plane resolution, SENSE factor = 2) were used to acquire 380 whole-brain volumes (36 slices, 3.5 mm slice thickness, .5 mm gap, anterior commissure-posterior commissure plane). A high-resolution three-dimensional image of the whole brain was acquired with a magnetization-prepared rapid gradient echo sequence (160 sagittal slices, echo time = 4.6 msec, repetition time = 9.9 msec, flip angle = 8°, voxel size = 1 × 1 × 1 mm). Functional data were acquired in two runs, each consisting of 40 seconds of resting fixation, followed by continuous presentation of the SELF or OTHER condition, followed by 40 seconds of resting fixation. The second scan consisted of the same parameters; condition order was counterbalanced across participants. Visual stimuli were presented using Cedrus Superlab 4.0.2 (San Pedro, California) viewable by a back projection screen.

Posttask Assessments

Following scanning, experimenters pretended to deliver electric shocks to the participants and manually logged heart rate responses, serving as an objective manipulation check for physiological responses to the possibility of being shocked (Supplementary Methods in Supplement 1) and to preserve the cover story until after the postquestionnaires had been administered. After scanning, participants completed a questionnaire assessing their belief in the cover story, reported effort placed into controlling the lines, self-reported anxiety about shocks, and strategies invoked during the task (Supplementary Methods in Supplement 1 for questions). At the conclusion of the experiment, participants were fully debriefed.

fMRI Analysis

Processing of fMRI data took place in Statistical Parametric Mapping 2 (SPM2, London, United Kingdom) (37). Preprocessing steps were carried out including slice time correction, motion correction, correction of movement-by-susceptibility interactions (38), and spatial normalization. Normalized functional data were spatially smoothed (6 mm full-width at half maximum Gaussian kernel).

Time points were categorized based on the height of the line as low (values 3–5), medium (values 5–7), high (values 7–9), and shock (values >9), with each level represented by a regressor for SELF and OTHER conditions and rest blocks serving as an implicit baseline. Regressors were convolved with the canonical hemodynamic response function to represent task effects. Task regressors were submitted to an individual subject voxelwise general linear model along with nuisance regressors (session mean, run regressor, linear trend, and six movement parameters derived from realignment corrections) to compute parameter estimates (β) and contrast images (containing weighted parameter estimates) for each comparison at each voxel. Because low-frequency drift artifacts were accounted for in the general linear model, high pass filtering was not performed.

Region-of-Interest Analysis

Random effects group analysis was carried out by defining regions of interest (ROIs) from an omnibus task > rest contrast unbiased with respect to condition and individual difference effects and subsequently testing ROIs for task and anxiety effects. As prior research has implicated the ventral basal forebrain consistent with the BNST, the medial temporal lobe and prefrontal structures in mediating threat and anxiety processing (22,24,39), we restricted ROI analyses to these regions. Nine spheres (4 mm radius in subcortical regions, 8 mm in cortical regions) were centered on task > rest activation peaks, thresholded at $p < .05$, corrected (whole-brain false discovery rate [FDR] corrected with five voxel minimum cluster size; Table 1).

Contrast coefficients were extracted from each region and submitted to a 2 (SELF, OTHER) × 4 (height: low, medium, high, shock) repeated-measures analysis of variance with anxiety as a

Table 1. Summary of ROI Results

Region	Talairach Coordinates			Proximity to Threat	Anxiety	Proximity to Threat × Anxiety
	x	y	z			
Left Amygdala	–33	–7	–15	.024	—	—
Right Amygdala	27	–7	–17	—	—	—
Left VBF/BNST	–9	0	–8	<.001•	.007	.012
Right VBF/BNST	12	–1	–10	—	—	—
Left DLPFC (BA 44)	–53	10	33	<.001•	—	<.001•
Right DLPFC (BA 44)	53	13	24	<.001•	—	.002•
Left Insula	–36	17	–8	—	—	—
Right Insula	45	20	–11	<.001•	—	.004•
DMPFC (BA 8)	6	37	40	<.001•	—	—

Regions listed were defined from an omnibus task > rest contrast and tested for proximity to threat, line condition, and anxiety effects within 2 (line type; SELF vs. OTHER) × 4 (proximity to threat; low, medium, high, shock) analyses of variance with anxiety as a continuous covariate. Values denote significance levels for main effects of proximity to threat and anxiety and the proximity to threat by anxiety interaction. No region demonstrated a significant main effect of line type, though the left insula trended toward greater response to the SELF relative to OTHER line ($p = .06$), see Figure 5. The p values marked with • denote those exceeding Bonferroni-adjusted significance threshold correcting for number of regions tested.

BA, Brodmann area; BNST, bed nucleus of the stria terminalis; DLPFC, dorsolateral prefrontal cortex; DMPFC, dorsal medial prefrontal cortex; ROI, region of interest; VBF, ventral basal forebrain.

continuous between-subject covariate. To facilitate visualization of individual difference effects, data were graphed as a function of anxiety based on a median split. As line height effects were observed to be linear, we calculated the slope of a regression line fit to the fMRI response to line height increases within each participant. Regression coefficients represent the slope of response as proximity to shock threshold increased and were tested against the continuous measure of anxiety using bivariate correlations. For the ROI-based group analysis, regions exceeding Bonferroni-corrected thresholding adjusting for number of ROIs tested are denoted with • in Table 1. All coordinates are reported in Talairach and Tournoux atlas space (40) and subcortical ROIs were localized using a detailed atlas of subcortical structures (41).

Whole-Brain fMRI Analysis

The ROI analysis was supplemented with a whole-brain analysis aimed at identifying additional brain regions whose activity was significantly modulated by threat proximity and anxiety. This analysis offers additional information regarding the spatial specificity of anxiety modulations that complement targeted ROI analyses. A conjunction analysis was used to generate a statistical map of brain activity showing both a linear increase in response as a function of line height and significantly exaggerated responsivity in more anxious participants. First, an inclusive mask was generated ($p < .05$, whole-brain FDR corrected, five voxel minimum cluster size) of brain areas showing a linear increase in activity with increasing proximity to threat (contrasts weights of -3 , -1 , 1 , and 3 for low, medium, high, and shock conditions, collapsed across SELF and OTHER). Within this mask, voxels were submitted to a regression with anxiety score as a between-subjects covariate, identifying areas showing larger linear-increasing responses to line height with greater anxiety. Anxiety effects exceeded a Bonferroni corrected threshold of $p < .05$ stipulated by Monte Carlo simulations conducted with the Alphasim plugin of Analysis of Functional Neuroimages software (Washington, DC) (42) based on the mask search volume.

To identify brain regions sensitive to controllability, a whole-brain paired-samples t test was conducted to identify brain areas showing differential activity to the SELF versus OTHER condition, thresholded at $p < .05$, whole-brain FDR corrected, five voxel minimum cluster size.

Results

Behavioral Results

Posttest results validated the task manipulation. Participants believed that the SELF condition better represented their own internal state [GSR: $F(1,46) = 15.07$, $p < .001$; fMRI: $F(1,48) = 12.15$, $p < .001$], reported having more success in controlling the SELF line [GSR: $F(1,46) = 45.57$, $p < .001$; fMRI: $F(1,48) = 7.28$, $p = .01$], and tried harder to control the SELF line [GSR: $F(1,46) = 171.34$, $p < .001$; fMRI: $F(1,48) = 132.06$, $p < .001$] relative to the OTHER line. Participants reported being equally nervous about earning shocks in the SELF and OTHER conditions (p 's $> .1$), indicating the two conditions were equated on subjectively experienced anxiety. The fMRI cohort yielded a significant main effect of anxiety on reported nervousness about shocks, with greater anxiety predicting higher overall nervousness ratings [$F(1,48) = 6.44$, $p = .014$].

Psychophysiological Results

Skin conductance data yielded a significant main effect of line height [$F(3,135) = 43.01$, $p < .001$], such that increasing line height predicted more frequent nonspecific skin conductance responses (NS-SCRs), best described by a linear function. We also observed a significant main effect of anxiety [$F(1,45) = 5.37$, $p < .05$], with higher anxiety predicting more frequent NS-SCRs. These effects were qualified by a line height by anxiety interaction [$F(3,135) = 3.01$, $p < .05$], with higher anxiety predicting an exaggerated increasing NS-SCR response to increasing line height (Figure 2C). This was additionally demonstrated by calculating the regression line best fitting each individual's NS-SCR frequency to increasing line height and correlating the slope of that line with anxiety scores [$r(46) = .30$, $p < .05$; Figure 3C]. The fMRI cohort demonstrated significantly elevated heart rate responses while expecting to be shocked following the task (Supplementary Results in Supplement 1).

Imaging Results

ROIs. Of the ROIs tested, six demonstrated significant proximity to threat and/or anxiety effects that survived Bonferroni correction (Table 1). Regions showing significant linear increases in activity with proximity to threat include the left VBF/BNST [$F(3,144) = 5.9$, $p = .001$; Figure 2A], the right insula [$F(3,144) = 12.4$, $p < .001$; Figure 2B], the left and right dorsolateral prefrontal cortex (DLPFC) [left: $F(3,144) = 21.0$, $p < .001$; right: $F(3,144) = 9.1$, $p < .001$; Figure S2A, B in Supplement 1], and the dorsal medial prefrontal cortex [$F(3,144) = 8.6$, $p < .001$]. The VBF/BNST also showed a significant main effect of anxiety, with enhanced recruitment in more anxious participants [$F(1,48) = 7.8$, $p < .01$; Figure 2A]. No regions demonstrated differential activity based on line type (SELF vs. OTHER; p 's $> .1$).

The left VBF/BNST, right insula, and the bilateral DLPFC demonstrated a significant line height by anxiety interaction [VBF/BNST: $F(3,144) = 3.8$, $p < .05$; right insula: $F(3,144) = 4.6$, $p < .005$; left DLPFC: $F(3,144) = 11.7$, $p < .001$; right DLPFC: $F(3,144) = 5.2$, $p < .005$; Figure 2A,B; Figure S2A, B in Supplement 1]. Specifically, greater anxiety predicted heightened engagement with increasing proximity to threat. See Supplementary Results in Supplement 1 for tests of a functional dissociation between VBF/BNST and amygdala response patterns.

As a second way to test the relationship between anxiety and line height response, we conducted correlation analyses to determine whether anxiety scores linearly predict the rise of an individual's response to increasing line height. Four regions demonstrated a significant positive relationship between anxiety and line height responding [left VBF/BNST: $r(49) = .33$, $p < .05$; right insula: $r(49) = .38$, $p < .01$; left DLPFC: $r(49) = .57$, $p < .001$; right DLPFC: $r(49) = .44$, $p < .005$; Figure 3A, B; Figures S3 and S4 in Supplement 1]. In cases where extreme outliers (defined as more than three interquartile ranges above the third or below the first quartile value) were present (VBF/BNST: four outliers, and right DLPFC: three outliers), removal improved the resulting correlations [VBF/BNST: $r(45) = .50$, $p < .001$; DLPFC: $r(46) = .47$, $p < .001$]. See Supplement 1 for results and discussion of time effects (early vs. late scan) on line height response.

Whole-Brain Analyses. Results of the conjunction analysis identifying brain regions that demonstrate a linear increasing line height response that was additionally exaggerated as function of greater trait anxiety included the left VBF/BNST [$xyz = -9, 0, -3$; $t(49) = 4.33$, $p < .05$, corrected], the right insula [$xyz = 56, 12, -1$; $t(49) = 4.02$, $p < .05$, corrected], the left and right anterior

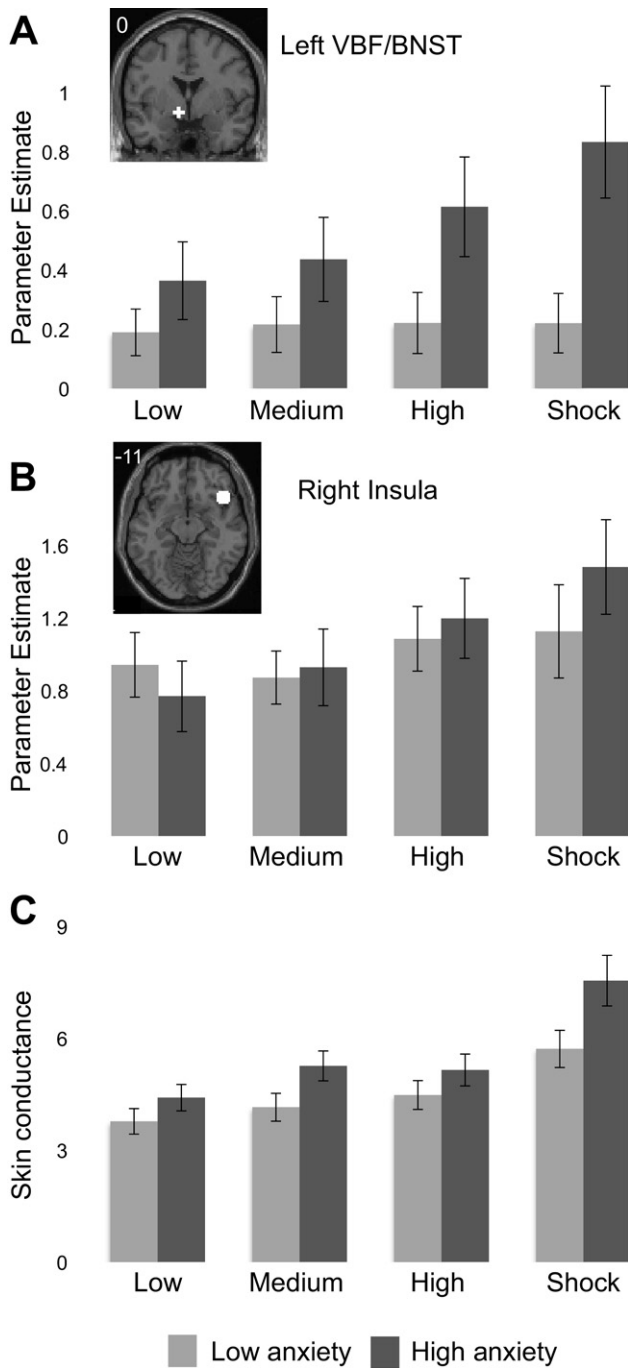


Figure 2. The VBF/BNST (A) and insula (B) were sensitive to increasing line height, with exaggerated responses in more anxious individuals. Line height represents a continuous stimulus that fluctuated in height, with greater height representing subsequent risk for receiving electric shocks. Shock is the maximum height, indicating a shock has been accumulated to be received later. Spherical regions of interest (white) were defined by an unbiased task > rest contrast and are depicted on a representative high-resolution anatomical image. Number in image represents the in-plane slice number in Talairach and Tournoux (41) atlas space. (C) Line height and anxiety modulated skin conductance responses. Line height is represented on the x axis and rate of nonspecific skin conductance responding, a measure of autonomic arousal in continuous stimulus paradigms, is represented on the y axis in response rate per minute. Anxiety groups are based on a median split of component scores for ease of presentation, though all statistical tests treat anxiety as a continuous variable. Error bars denote standard error of the mean. Image presented in left = left coordinate space. BNST, bed nucleus of the stria terminalis; VBF, ventral basal forebrain.

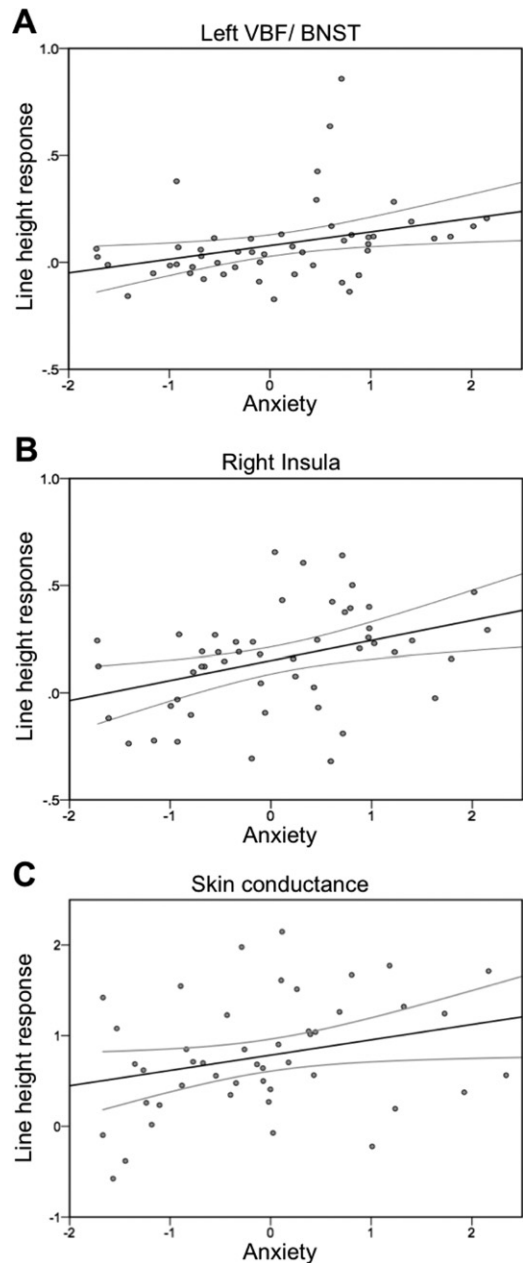


Figure 3. Anxiety predicts line height response in the left VBF/BNST (A), right insula (B), and skin conductance response rates (C). Regions in (A) and (B) are viewable in Figure 2. The x axis represents anxiety based on component scores and the y axis represents the slope of the regression line representing increasing functional magnetic resonance imaging responses (A,B) or nonspecific skin conductance responses rates (C) with increasing proximity to threat. Black line denotes regression fit line and gray lines represent 95% confidence intervals of the mean. BNST, bed nucleus of the stria terminalis; VBF, ventral basal forebrain.

ventrolateral prefrontal cortex [xyz = -56,13,30; $t(49) = 4.24$, $p < .05$, corrected; xyz = 48,46,-5; $t(49) = 3.62$, $p < .05$, corrected], and the left and right DLPFC [xyz = -47,-7,45; $t(49) = 4.09$, $p < .05$, corrected; xyz = 30,-1,47; $t(49) = 4.52$, $p < .05$, corrected; Figure 4]. For a full list of activations, Table S2 in Supplement 1.

A whole-brain analysis (SELF vs. OTHER) exploring differences in locus of control revealed a single region, the right

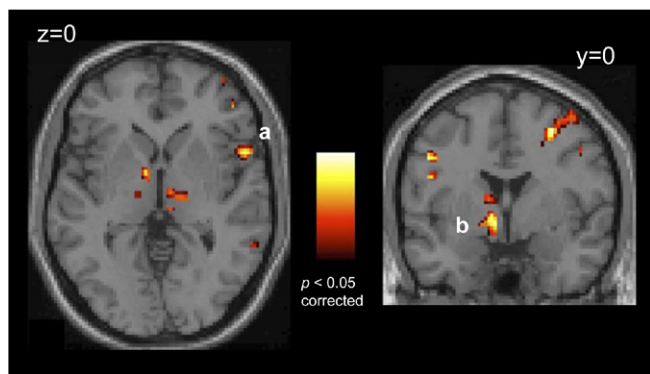


Figure 4. Converging evidence from whole-brain analyses implicates the insula (a) and ventral basal forebrain/bed nucleus of the stria terminalis (b) in representing hypervigilant threat monitoring with greater trait anxiety. Statistical maps show results of a conjunction analysis representing images demonstrating both a linearly increasing response as a function of line height ($p < .05$, whole-brain false discovery rate corrected) and significantly exaggerated responsivity in more anxious individuals ($p < .05$, corrected). Activations are displayed on a representative high-resolution anatomical image. Number in image represents the in-plane slice number in Talairach and Tournoux (41) atlas space. Image presented in left = left coordinate space.

anterior insula [$xyz = 42,11,-11$; $t(49) = 6.17$, $p < .05$, corrected, Figure 5], with greater activity in the SELF than the OTHER condition. No region showed greater activity to the OTHER condition than the SELF condition. See Supplement 1 for discussion of this effect.

Discussion

These experiments aimed to characterize putative neural bases of hypervigilant threat monitoring across a broad spectrum of healthy trait anxiety levels. Using a continuous paradigm validated to invoke differential arousal based on threat proximity, we observed that the left VBF/BNST, right insula, and lateral cortical regions tracked proximity to the shock threshold. Further, these responses were exaggerated in more dispositionally anxious participants. Together with prior work, the current findings implicate these regions in representing the kinds of exaggerated vigilant threat-monitoring behaviors characteristic of anxious individuals (1).

Based on physiological and self-report assessments, participants experienced the task as intended. Physiological indices of arousal increased with increasing line height as measured by skin conductance responses, and fMRI participants demonstrated a heightened heart rate response in anticipation of shock delivery postscanning. Moreover, more trait anxious individuals demonstrated exaggerated skin conductance responding and an exaggerated heart rate increase. These findings converge with prior work reporting greater physiological responses to aversive cues in individuals with higher anxiety (43,44) and in anxiety disorders (6,45,46). In this paradigm, the height of the line served as an environmental cue providing relevant information to an individual's future relative level of threat or safety. The VBF/BNST, insular cortex, and lateral prefrontal cortex demonstrated both a linear increase in response as line height increased and exaggerated activity in more anxious individuals. Taken together, these data implicate these regions in exaggerated continuous environmental threat monitoring with greater trait anxiety.

The BNST, located dorsal, medial, and anterior to the amygdala and adjacent to the anterior commissure, is a ventral

forebrain structure that like the central nucleus of the amygdala (CN), projects to the brainstem and hypothalamus to mediate arousal and stress responses (47,48). The similarity in these projections has led anatomists to consider the BNST an extension of the CN, the so-called “extended amygdala” (49). In terms of neurochemical and cellular makeup, the BNST holds many similarities to the CN (50) but also possesses some key anatomical differences that may be critical to their divergent functional profiles. The BNST is especially sensitive to corticotropin releasing factor (51–53), a neuropeptide mediating long-lasting peripheral stress responses (54). In the temporal trajectory of threat processing, the basolateral amygdala drives immediate, phasic emotional responses (55), whereas temporally extended changes in arousal are represented in activity of the BNST (56). This shift is likely mediated by direct connections between the basolateral amygdala and BNST (57) and the hippocampus and BNST (58,59), given the role of the latter brain structure in monitoring context (60). The involvement of the VBF/BNST in the present task is consistent with its role in representing temporally diffuse and extended vigilance states (61) related to environmental monitoring. This conception converges with other recent work implicating forebrain and midbrain regions in representing the imminence of potential threats (62).

Given the unique neuroanatomical properties of the ventral basal forebrain, care should be taken in drawing definitive conclusions regarding the contribution of the BNST versus neighboring nuclei in the reported effects. Within the ventral basal forebrain, cell groups from multiple structures are comingled (63,64), rendering their boundaries unclear and motivating our labeling of the observed effects VBF/BNST. However, when referencing the location of the observed VBF activations to a detailed subcortical human brain atlas (41), activations localized within the boundaries of the BNST (Figure S4 in Supplement 1). Future research with converging and higher resolution methodologies may provide additional confidence in the role of the human BNST in vigilance and anxiety processes.

The amygdala plays a key functional role in processing salient cues that predict affective environmental events (22,23,65–67)

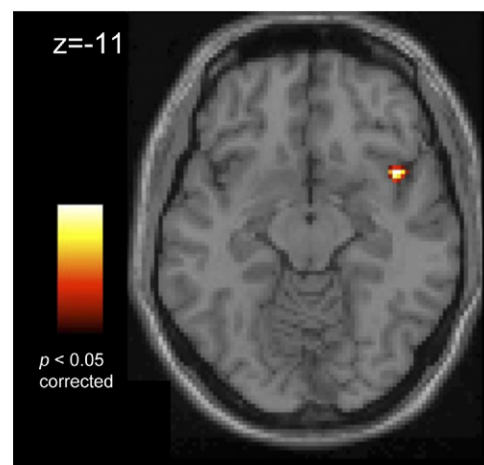


Figure 5. The right insula shows significantly greater activity when viewing a stimulus line thought to represent one's own physiological state, compared with passively viewing someone else's physiological state ($p < .05$, whole-brain false discovery rate corrected). Images displayed on a representative high-resolution anatomical image. Number in image represents the in-plane slice number in Talairach and Tournoux (41) atlas space. Image presented in left = left coordinate space.

and has shown cued hyperresponding in anxiety disorders (24,68,69). However, in this study, the amygdala showed minimal task-modulated activity or anxiety modulation even at exploratory thresholds. Weak amygdala engagement underscores the importance of considering the experimental context when interpreting neuroimaging findings and highlights key differences between the present experimental context and prior work (70–72). In this study, threat level varied slowly along continuous dimensions, and the task was devoid of transient affective events. In contrast, typical provocation paradigms present discrete threatening cues (e.g., threatening face, conditioned stimulus) and measure the short-duration hemodynamic responses that follow. The continuous line stimulus, devoid of transient cues, enables measurement of sustained variation of neural responses to which provocation paradigms are typically insensitive. Further work utilizing experimental paradigms with both transient and continuous manipulations may provide additional evidence to support a functional distinction between the amygdala and other regions such as the BNST and insula in affective processing along different time scales.

In addition to the VBF/BNST, we observed similar task and trait anxiety modulation of activity within the insular cortex. The insular cortex has been implicated in anticipatory and overt affective processing in healthy individuals (73–77), with hyperresponsivity in individuals with high trait anxiety (78) and in anxiety disorders (24). These findings have led some to suggest the insular cortex plays a key role in anxiety by integrating afferent inputs from subcortical regions (79) with body state information, which may be exaggerated in clinically anxious individuals leading to enhanced autonomic output and physiological hyperarousal (80). Taken with the present results, the insula may be responsive to both transient threat cues as well as extended threat contexts, consistent with a proposed superordinate role for this region in mediating autonomic arousal (81).

We also observed heightened engagement of lateral prefrontal regions in response to increasing threat proximity, with hyperrecruitment in more dispositionally anxious individuals. At first glance, these results seem contrary to work implicating lateral prefrontal regions in disengaging from threatening cues to perform a secondary task (82–84), a behavior in which trait anxious individuals show deficits (85). However, other studies have demonstrated enhanced recruitment of lateral prefrontal regions while anticipating aversive events (86–88). Though speculative, differences in task demands may partially explain these discrepant effects. Whereas divided attention paradigms draw on cognitive resources to disengage attention from affective cues, contexts involving straightforward anticipation may leave these same cognitive resources free to generate ruminative cognitions. If correct, this interpretation predicts diminished recruitment in anxious individuals in disengagement contexts and exaggerated recruitment in anxious individuals in anticipatory contexts. The present findings support this distinction and suggest that anticipatory responses mediated by the lateral prefrontal cortex can be continuous in time scale and upregulated by trait anxiety.

Identifying the neural representation of continuous threat monitoring may have particular relevance to anxiety disorders, a class of Axis I psychiatric illness (4). Some anxiety disorders have been theorized as disorders of “hyperfear” processing, namely exaggerated responses to clearly defined external cues (e.g., phobias), whereas others are characterized by a diffuse pattern of physiological arousal and negative affect (e.g., generalized anxiety disorder) (2,18,89) and most anxiety disorders are marked by

interactions among both processes. The present findings suggest that the neurobiological mechanisms subserving these key features of anxiety are at least partially distinct. The BNST, though implicated in animal models of anxiety, has not been widely reported in neuroimaging experiments testing anxiety disorder samples (90) and was not detected in a meta-analysis of exaggerated responses in clinically anxious populations (24). This initial experiment offers the suggestion that the VBF/BNST plays a role in sustained anxiety symptoms in humans that may not be detectable in the preponderance of experiments to date manipulating cued affect. These findings motivate the hypothesis that anxiety symptoms characterized by temporally extended threat monitoring are mediated by exaggerated responding in brain regions such as the VBF/BNST. Assessing brain mechanisms that support continuous changes in environmental threat monitoring may inform new circuitries mediating pathological sustained anxious behaviors.

This work was supported by a National Science Foundation Graduate Research Fellowship (LHS); postdoctoral support for LHS from DA007274, NSF0746220 (WMK), MH080716 (PJW); and the Dartmouth Brain Imaging Center.

We gratefully acknowledge Kathryn Demos, Tammy Moran, Maital Neta, and Courtney Rogers for assistance with data acquisition; M. Justin Kim, Dylan David Wagner, Gagan Wig, and George Wolford for assistance with data analysis; Natasha Mehta for assistance with figure preparation; and B.J. Casey, F. Caroline Davis, Todd Heatherton, Catherine Norris, and Lisa Shin for helpful discussion.

The authors reported no biomedical financial interests or potential conflicts of interest.

Supplementary material cited in this article is available online.

1. Eysenck M (1992): *Anxiety: The Cognitive Perspective*. Hillsdale, NJ: Erlbaum.
2. Rosen JB, Schulkin J (1998): From normal fear to pathological anxiety. *Psychol Rev* 105:325–350.
3. Thayer JF, Friedman BH, Borkovec TD (1996): Autonomic characteristics of generalized anxiety disorder and worry. *Biol Psychiatry* 39:255–266.
4. American Psychiatric Association (1994): *Diagnostic and Statistical Manual of Mental Disorders*. Washington, DC: American Psychiatric Association.
5. Lang PJ, Davis M, Ohman A (2000): Fear and anxiety: Animal models and human cognitive psychophysiology. *J Affect Disord* 61:137–159.
6. Grillon C (2008): Models and mechanisms of anxiety: Evidence from startle studies. *Psychopharmacology (Berl)* 199:421–437.
7. Barlow DH (2001): Unraveling the mysteries of anxiety and its disorders from the perspective of emotion theory. *Am Psychol* 55:1247–1263.
8. Bar-Haim Y, Lamy D, Pergamin L, Bakerman-Kranenburg MJ, van Izenendoorn MH (2007): Threat-related attentional bias in anxious and non-anxious individuals: A meta-analytic study. *Psychol Bull* 133:1–24.
9. Mathews A, Mackintosh B, Fulcher EP (1997): Cognitive biases in anxiety and attention to threat. *Trends Cogn Sci* 1:340–345.
10. Walker DL, Toufexis DJ, Davis M (2003): Role of the bed nucleus of the stria terminalis versus the amygdala in fear, stress, and anxiety. *Eur J Pharmacol* 463:199–216.
11. Davis M, Walker DL, Lee Y (1997): Amygdala and bed nucleus of the stria terminalis: Differential roles in fear and anxiety measured with the acoustic startle reflex. *Ann N Y Acad Sci* 821:305–331.
12. Blanchard RJ, Yudko EB, Rodgers RJ, Blanchard DC (1993): Defense system psychopharmacology: An ethological approach to the pharmacology of fear and anxiety. *Behav Brain Res* 58:155–165.
13. Fanselow MS (1994): Neural organization of the defensive behavior system responsible for fear. *Psychon Bull Rev* 1:429–438.

14. Hitchcock JM, Davis M (1986): Lesions of the amygdala, but not of the cerebellum or red nucleus, block conditioned fear as measured with the potentiated startle paradigm. *Behav Neurosci* 100:11–22.
15. Hitchcock JM, Davis M (1991): The efferent pathway of the amygdala involved in conditioned fear as measured with the fear-potentiated startle paradigm. *Behav Neurosci* 105:826–842.
16. leDoux JE, Iwata J, Cicchetti P, Reis DJ (1988): Different projections of the central amygdaloid nucleus mediate autonomic and behavioral correlates of conditioned fear. *J Neurosci* 8:2517–2529.
17. Hammack SE, Richey KJ, Watkins LR, Maier SF (2004): Chemical lesion of the bed nucleus of the stria terminalis blocks the behavioral consequences of uncontrollable stress. *Behav Neurosci* 118:443–448.
18. Davis M (1999): The extended amygdala: Are the central nucleus of the amygdala and the bed nucleus of the stria terminalis differentially involved in fear versus anxiety? *Ann N Y Acad Sci* 29:281–291.
19. Oler JA, Fox AS, Shelton SE, Christian BT, Murali D, Oakes TR, *et al.* (2009): Serotonin transporter availability in the amygdala and bed nucleus of the stria terminalis predicts anxious temperament and brain glucose metabolic activity. *J Neurosci* 29:9961–9966.
20. Fox AS, Shelton SE, Oakes TR, Davidson RJ, Kalin NH (2008): Trait-like brain activity during adolescence predicts anxious temperament in primates. *PLoS ONE* 3:e2570.
21. Durvarci S, Bauer EP, Paré D (2009): The bed nucleus of the stria terminalis mediates inter-individual variations in anxiety and fear. *J Neurosci* 29:10357–10361.
22. Costafreda SG, Brammer MJ, David AS, Fu CHY (2007): Predictors of amygdala activation during the processing of emotional stimuli: A meta-analysis of 385 PET and fMRI studies. *Brain Res Rev* 58:57–70.
23. Kober H, Barrett LF, Joseph J, Bliss-Moreau E, Lindquist K, Wager TD (2008): Functional grouping and cortical-subcortical interactions in emotion: A meta-analysis of neuroimaging studies. *Neuroimage* 42:998–1031.
24. Etkin A, Wager TD (2007): Functional neuroimaging of anxiety: A meta-analysis of emotional processing in PTSD, social anxiety disorder, and specific phobia. *Am J Psychiatry* 164:1476–1488.
25. Shin LM, Rauch SL, Pitman RK, Whalen PJ (2009): The human amygdala in anxiety disorders. In: Phelps EA, Whalen PJ, editors. *The Human Amygdala*. New York: Guilford Publications.
26. Vogelanz ND, Hecker JE (1999): The roles of neuroticism and controllability/predictability in physiological responses to aversive stimuli. *Pers Individ Dif* 27:599–612.
27. First MB, Spitzer MRI, Williams JBW, Gibbon M (1995): *Structured Clinical Interview for DSM-IV (SCID)*. Washington, DC: American Psychiatric Association.
28. Beck AT, Ward CH, Mendelson M, Mock J, Erbaugh J (1961): An inventory for measuring depression. *Arch Gen Psychiatry* 4:561–571.
29. Oldfield RC (1971): The assessment and analysis of handedness: The Edinburgh Inventory. *Neuropsychologia* 9:97–113.
30. Spielberger CD, Gorsuch RL, Lushene RE (1988): *STAI-Manual for the State Trait Anxiety Inventory, 3rd ed.* Palo Alto, CA: Consulting Psychologists Press.
31. Carver CS, White TL (1994): Behavioral inhibition, behavioral activation, and affective responses to impending reward and punishment: The BIS/BAS scales. *J Pers Soc Psychol* 67:319–333.
32. Costa PT, McCrae RR (1991): *NEO Five-Factor Inventory (NEO-FFI) Professional Manual*. Odessa, FL: Psychological Assessment Resources.
33. Buhr K, Dugas MJ (2002): The Intolerance of Uncertainty Scale: Psychometric properties of the English version. *Behav Res Ther* 40:931–945.
34. Meyer TJ, Miller ML, Metzger RL, Borkovec TD (1990): Development and validation of the Penn State Worry Questionnaire. *Behav Res Ther* 28:487–495.
35. Peterson RA, Reiss S (1987): *Test Manual for the Anxiety Sensitivity Index*. Orland Park, IL: International Diagnostic Systems.
36. Stevens J (2007): *Applied Multivariate Statistics for the Social Sciences*. Mahwah, NJ: Lawrence Erlbaum Associates.
37. Friston KJ, Holmes A, Worsley K, Poline J, Frith C, Frackowiak R (1995): Statistical parametric maps in functional imaging: A general linear approach. *Hum Brain Mapp* 2:189–210.
38. Andersson JLR, Hutton C, Ashburner J, Turner R, Friston K (2001): Modeling geometric deformations in EPI time series. *Neuroimage* 13:903–919.
39. Bishop SJ (2007): Neurocognitive mechanisms of anxiety: An integrative account. *Trends Cogn Sci* 11:307–316.
40. Talairach J, Tournoux P (1988): *Co-Planar Stereotaxic Atlas of the Human Brain*. New York: Thieme Medical Publishers.
41. Mai JK, Assheuer J, Paxinos G (1997): *Atlas of the Human Brain*. San Diego: Academic Press.
42. Cox RW (1996): AFNI: Software for analysis and visualization of functional magnetic resonance neuroimages. *Comput Biomed Res* 29:162–173.
43. Norris CJ, Larsen JT, Cacioppo JT (2007): Neuroticism is associated with larger and more prolonged electrodermal responses to emotionally evocative pictures. *Psychophysiology* 44:823–826.
44. Mardaga S, Laloyaux O, Hansenne (2006): Personality traits modulate skin conductance response to emotional pictures: An investigation with Cloninger's model of personality. *Pers Individ Dif* 40:1603–1614.
45. Grillon C, Ameli R, Goddard A, Woods S, Davis M (1994): Baseline and fear-potentiated startle in panic disorder patients. *Biol Psychiatry* 35:431–439.
46. Grillon C, Morgan CA (1999): Fear-potentiated startle conditioning to explicit and contextual cues in gulf war veterans with posttraumatic stress disorder. *J Abnorm Psychol* 108:134–142.
47. Herman DH, Cullinan WE (1997): Neurocircuitry of stress: Central control of hypothalamo-pituitary-adrenocortical axis. *Trends Neurosci* 20:78–84.
48. Berntson GG, Sarter M, Cacioppo JT (1998): Anxiety and cardiovascular reactivity: The basal forebrain cholinergic link. *Behav Brain Res* 94:225–248.
49. Alheid GF, Heimer L (1988): New perspectives in basal forebrain organization of special relevance for neuropsychiatric disorders: The striato-pallidal, amygdaloid, and corticopetal components of substantia innominata. *Neuroscience* 27:1–39.
50. Alheid GF, deOlmos JS, Beltramini CA (1995): Amygdala and extended amygdala. In: Paxinos G, editor. *The Rat Nervous System*. New York: Academic Press.
51. de Jongh R, Groenink L, van der Gugten J, Olivier B (2003): Light-enhanced and fear-potentiated startle: Temporal characteristics and effects of alpha-helical corticotropin-releasing hormone. *Biol Psychiatry* 54:1041–1048.
52. Lee Y, Davis M (1997): Role of the hippocampus, bed nucleus of the stria terminalis and amygdala in the excitatory effect of corticotropin releasing hormone on the acoustic startle reflex. *J Neurosci* 17:6434–6446.
53. Liang KC, Melia KR, Miserendino MJD, Falls WA, Campeau S, Davis M (1992): Corticotropin releasing factor: Long-lasting facilitation of the acoustic startle reflex. *J Neurosci* 12:2303–2312.
54. Dunn AJ, Berridge CW (1990): Physiological and behavioral responses to corticotropin-releasing factor administration: Is CRF a mediator of anxiety or stress responses. *Brain Res Rev* 15:71–100.
55. leDoux JE, Cicchetti P, Xagoraris A, Romanski LM (1990): The lateral amygdaloid nucleus: Sensory interface of the amygdala in fear conditioning. *J Neurosci* 10:1062–1069.
56. Waddell J, Morris RW, Bouton ME (2006): Effects of bed nucleus of the stria terminalis lesions on conditioned anxiety: Aversive conditioning with long-duration conditional stimuli and reinstatement of extinguished fear. *Behav Neurosci* 120:324–336.
57. Dong H-W, Petrovich GD, Swanson LW (2001): Topography of projections from amygdala to bed nuclei of the stria terminalis. *Brain Res Rev* 38:192–246.
58. Pitkänen A, Pikkarainen M, Nurminen N, Ylinen A (2000): Reciprocal connections between the amygdala and the hippocampal formation, perirhinal cortex, and postrhinal cortex in rat: A review. *Ann N Y Acad Sci* 911:369–391.
59. Van Groen T, Wyss JM (1990): Extrinsic projections from area CA1 of the rat hippocampus: Olfactory, cortical, subcortical, and bilateral hippocampal formation projections. *J Comp Neurol* 302:515–528.
60. Phillips RG, leDoux JE (1992): Differential contribution of the amygdala and hippocampus to cued and contextual fear conditioning. *Behav Neurosci* 106:274–285.
61. Walker DL, Miles LA, Davis M (2009): Selective participation of the bed nucleus of the stria terminalis and CRF in sustained anxiety-like versus phasic fear-like responses. *Prog Neuropsychopharmacol Biol Psychiatry* 33:1291–1308.
62. Mobbs D, Petrovic P, Marchant JL, Hassabis D, Weiskopf N, Seymour B, *et al.* (2007): When fear is near: Threat imminence elicits prefrontal-periaqueductal gray shifts in humans. *Science* 317:1079–1083.

63. de Olmos JS, Heimer L (1999): The concepts of the ventral striatopallidal system and extended amygdala. *Ann N Y Acad Sci* 877:1–32.
64. Whalen PJ, Davis FC, Oler JA, Kim H, Kim MJ, Neta M (2009): Human amygdala responses to facial expressions of emotion. In: Whalen PJ, Phelps EA, editors. *The Human Amygdala*. New York: Guilford Publications.
65. LeDoux JE (2000): Emotion circuits in the brain. *Annu Rev Neurosci* 23:155–184.
66. Phelps EA (2006): Emotion and cognition: Insights from studies of the human amygdala. *Annu Rev Psychol* 57:27–53.
67. Davis M, Whalen PJ (2001): The amygdala: Vigilance and emotion. *Mol Psychiatry* 6:13–34.
68. Rauch SL, Shin LM, Wright CI (2003): Neuroimaging studies of amygdala function in anxiety disorders. *Ann N Y Acad Sci* 985:389–410.
69. Rauch SL, Whalen PJ, Shin LM, McInerney SC, Macklin ML, Lasko NB, *et al.* (2000): Exaggerated amygdala response to masked facial stimuli in posttraumatic stress disorder: A functional MRI study. *Biol Psychiatry* 47:769–776.
70. Somerville LH, Kim H, Johnstone T, Alexander AL, Whalen PJ (2004): Human amygdala responses during presentation of happy and neutral faces: Correlations with state anxiety. *Biol Psychiatry* 55:897–903.
71. Etkin A, Klemenhagen KC, Dudman JT, Rogan MT, Hen R, Kandel ER, Hirsch J (2004): Individual differences in trait anxiety predict the response of the basolateral amygdala to unconsciously processed fearful faces. *Neuron* 44:1043–1055.
72. Hare TA, Tottenham N, Galvan A, Voss HU, Glover GH, Casey BJ (2008): Biological substrates of emotional reactivity and regulation in adolescence during an emotional go-nogo task. *Biol Psychiatry* 63:927–934.
73. Berns GS, Chappelow J, Cecic M, Zink CF, Pagnoni G, Martin-Skurski ME (2006): Neurobiological substrates of dread. *Science* 312:754–757.
74. Phelps EA, O'Connor KJ, Gatenby JC, Gore JC, Grillon C, Davis M (2001): Activation of the left amygdala to a cognitive representation of fear. *Nat Neurosci* 4:437–441.
75. Ploghaus A, Tracey I, Gati JS, Clare S, Menon RS, Matthews PM, Rawlins JN (1999): Dissociating pain from its anticipation in the human brain. *Science* 284:1979–1981.
76. Phan KL, Wager TD, Taylor SF, Liberzon I (2002): Functional neuroanatomy of emotion: A meta-analysis of emotion activation studies in PET and fMRI. *Neuroimage* 16:331–348.
77. Chua P, Krams M, Toni I, Passingham R, Dolan R (1999): A functional anatomy of anticipatory anxiety. *Neuroimage* 9:563–571.
78. Stein MB, Simmons AN, Feinstein JS, Paulus MP (2007): Increased amygdala and insula activation during emotion processing in anxiety-prone subjects. *Am J Psychiatry* 164:318–327.
79. McDonald AJ, Shamman-Lagnado SJ, Shi CJ, Davis M (1999): Cortical afferents to the extended amygdala. In: McGinty JF, editor. *Annals of the New York Academy of Sciences*. New York: New York Academy of Sciences, 309–338.
80. Paulus MP, Stein MB (2006): An insular view on anxiety. *Biol Psychiatry* 60:383–387.
81. Craig AD (2003): Interoception: The sense of the physiological condition of the body. *Curr Opin Neurobiol* 13:500–505.
82. Bishop SJ, Duncan J, Brett M, Lawrence AD (2004): Prefrontal cortical function and anxiety: Controlling attention to threat-related stimuli. *Nat Neurosci* 7:184–188.
83. Bishop SJ, Jenkins R, Lawrence AD (2007): Neural processing of fearful faces: Effects of anxiety are gated by perceptual capacity limitations. *Cereb Cortex* 17:1595–1603.
84. Bishop SJ (2009): Trait anxiety and impoverished prefrontal control of attention. *Nat Neurosci* 12:92–98.
85. Fox E, Russo R, Bowles R, Dutton K (2001): Do threatening stimuli draw or hold visual attention in subclinical anxiety? *J Exp Psychol Gen* 130:681–700.
86. Nitschke JB, Sarinopoulos I, Mackiewicz KL, Schaefer HS, Davidson RJ (2006): Functional neuroanatomy of aversion and its anticipation. *Neuroimage* 29:106–116.
87. Dalton KM, Kalin NH, Grist TM, Davidson RJ (2005): Neural-cardiac coupling in threat-evoked anxiety. *J Cogn Neurosci* 17:969–980.
88. Simmons A, Matthews SC, Stein MB, Paulus MP (2004): Anticipation of emotionally aversive visual stimuli activates right insula. *Neuroreport* 15:2261–2265.
89. Barlow DH (1988): *Anxiety and Its Disorders*. New York: Guilford Press.
90. Straube T, Mentzel H-J, Milner WHR (2007): Waiting for spiders: Brain activation during anticipatory anxiety in spider phobics. *Neuroimage* 37:1427–1436.